Published in final edited form as:
Neuroimage. 2008 August 15; 42(2): 611–616. doi:10.1016/j.neuroimage.2008.05.007.

Multi-site voxel-based morphometry: Methods and a feasibility demonstration with childhood absence epilepsy

Heath Pardoe[a], **Gaby S. Pell**[a], **David F. Abbott**[a,b], **Anne T. Berg**[c], and **Graeme D. Jackson**[a,b,*]

[a] Brain Research Institute, Florey Neuroscience Institutes (Austin), Melbourne, Australia

[b] The University of Melbourne, Parkville, Victoria, Australia

[c] Northern Illinois University, Department of Biology, De Kalb, IL 60115, USA

Abstract

Aim—Voxel-based morphometry analysis of neurological disorders would benefit if it could use data acquired from different scanners, but scanner based contrast variation could interfere with the detection of disease-specific structural abnormalities. In this study we examine MRI data from three different sites to investigate structural differences between childhood absence epilepsy (CAE) subjects and controls.

Methods—T1-weighted structural MRI scans were acquired from: Site A. 10 CAE, 213 controls; Site B. 15 CAE, 33 controls; and Site C. 19 CAE, 11 controls. The images were processed using the optimised VBM protocol. Three statistical analyses were undertaken: (1) Comparisons of CAE subjects and controls stratified by site. (2) Between-site comparison of controls from each site. (3) Factorial analysis of all data with site and disease status as factors.

Results—Consistent regions of structural change, located in the thalamic nuclei, were observed in the within-site analysis of CAE vs controls. Analysis of control scans, however, indicated site-specific differences between controls, which required that we adjust for site in combined analyses. Analysis of all data with adjustment for site confirmed the finding of thalamic atrophy in CAE cases.

Conclusion—Combined VBM analysis of structural MRI scans acquired from different sites yield consistent patterns of structural change in CAE when site is included as a factor in the statistical analysis of the processed images. In MRI studies of diseases where only a limited number of subjects can be imaged at each site, our study supports the possibility of effective multi-site studies as long as both disease subjects and healthy controls are acquired from each site.

Keywords

Voxel-based morphometry; Brain structure; Epilepsy; MRI

Introduction

Clinical studies recruiting subjects from multiple sites have always been a powerful way of studying disease. MRI is the imaging modality of choice to determine brain abnormalities associated with a neurological disorder. One of the most widely used objective techniques for the investigation of structural changes using MRI is voxel-based morphometry (VBM). However, the use of multiple imaging centres in MRI studies has been limited by concerns

*Corresponding author. Brain Research Institute, Neurosciences Building, Austin Health, Heidelberg West, Victoria 3081, Australia. Fax: +613 9496 2980. E-mail address: BRI@brain.org.au (G.D. Jackson).

over inter-site variability due to technical differences in MR scanner hardware and acquisition parameters.

The major problem is that differences between the scanners including field-strength effects, differences in imaging sequence parameters, radio-frequency (RF) coils and non-linear gradient fields may lead to regionally heterogenous contrast variation in the acquired MRI scans. These variations in contrast may specifically affect the VBM analysis and show changes in regions that cannot be distinguished from real biological effects associated with the disease being studied.

Childhood absence epilepsy (CAE) is a common form of childhood epilepsy that is easily recognized and thus ideally suited to studying inter-site variation as sufficient numbers of CAE subjects can be easily recruited at multiple sites. Typically, structural MRI's in these patients show no obvious abnormalities on visual inspection; however, subtle abnormalities, specifically statistically demonstrable thalamic atrophy have been revealed by quantitative analysis of groups of patients (Chan et al., 2006).

Our primary aim in this paper is to test the validity of using VBM to analyse images acquired at three sites imaged with different scanners, including different field strength, if we explicitly model the site as a factor in the statistical analysis of the acquired data. We use control MRI data from three different sites to determine site-specific variations due primarily to these technical factors. We investigate the relative magnitude of differences attributable to site factors as compared with differences due to the biology of CAE.

Methods

Subjects

At all three sites, the diagnosis of CAE was based on t he criteria of the International League Against Epilepsy classification of epilepsy syndromes (1989). It was applied by at least two experienced epileptologists at all sites as described in Chan et al. (2006) (Site A) and Berg et al. (1999) (Site B and Site C).

Site A (Austin Hospital, Australia)—10 subjects with CAE (9 female, 18±9 years) were recruited through the First Seizure Clinic, the EEG laboratory and the private practices of the clinical investigators. All CAE subjects had typical electroclinical features for CAE at the time of diagnosis. Mean age of onset of seizures was 6±3 years. The patients were scanned between 0–11 years after seizure onset. 213 controls (115 female, mean age 34±13 years) were imaged at the same site. All subjects, or their parent or guardian in the case of minors, gave written informed consent.

Site B (Yale Hospital, U.S.A.)—15 subjects with CAE (6 female, mean age 15±2 years) were recruited for the Connecticut Study of Epilepsy in Children (Berg et al., 2008). 33 controls (16 female, mean age 18±5 years) were imaged at the same site.

Site C (Hartford Children's Hospital, Connecticut, U.S.A.)—19 subjects with CAE (13 female, mean age 15±2 years) were recruited for the Connecticut Study of Epilepsy in Children (Berg et al., 2008). 11 controls (4 female, mean age 16±5 years) were imaged at the same site.

All controls were considered to be neurologically normal, without any history of epilepsy, neurologic disorders or other major medical illness, and written informed consent of adult subjects or written parental permission and assent of minor were obtained as required by the

Institutional Review Board of record at each site. Ethics approval for the scans of controls and patients were obtained from the relevant authorities.

MR imaging

Site A—Subjects were imaged on a 3T GE Signa LX whole-body scanner (General Electric, Milwaukee, WI, USA). A whole-brain T1-weighted coronal 3D fast spoiled gradient recovery (FSPGR) sequence was used (TE = 1.9ms, TR = 9ms, TI = 500ms, flip angle 20°, matrix size 512 × 256, FOV = 25 × 17.5cm, head transmit/receive coil) with contiguous coronal slices of 2mm thickness. All MRI scans were reviewed by an experienced neuroradiologist and reported as normal.

Site B—Subjects were imaged on a 1.5T Siemens Sonata MR scanner (Siemens, Erlangen, Germany). Structural MRI was obtained using a whole-brain T1-weighted coronal 3D MP-RAGE sequence acquisition (TE = 4.38ms, TR = 1730ms, TI = 1100ms, flip angle = 15°, matrix size = 256 × 256, FOV = 27cm, body transmit/head receive coil) with contiguous coronal slices of 1.6mm thickness. All MRI scans were reviewed by an experienced neuroradiologist and reported as normal.

Site C—Subjects were imaged on a 1.5T GE Signa MR scanner (General Electric, Milwaukee, WI, USA). A whole-brain T1-weighted coronal 3D spoiled gradient recovery (SPGR) sequence was used (TE = 2.64ms, TR = 13.76ms, TI = 450ms, flip angle = 20°, matrix size = 256 × 192, FOV = 27 × 18cm, head transmit/receive coil) with contiguous coronal slices of 1.6mm thickness. All MRI scans were reviewed by an experienced neuroradiologist and reported as normal.

Image analysis

Voxel-based morphometry—The acquired images were pre-processed using the optimised VBM protocol (Good et al., 2001). Unless otherwise specified, 10mm Gaussian FWHM smoothing was applied to the gray-matter segment and the smoothed, modulated gray-matter (GM) segments were compared. In all of the subsequent comparisons age, gender and total intracranial volume (TIV) are included as covariates in the analysis. TIV was calculated as the sum of the gray-matter (GM), white-matter (WM) and CSF segments, over the whole brain.

Individual site analyses: CAE and control data GM concentration images from each site were compared using a two-sample *t*-test. The resulting maps of the test statistic were thresholded at $p < 0.05$ uncorrected for multiple comparisons. This threshold was chosen to deliberately overestimate the number of voxels in which there are significant differences i.e. there are likely to be a number of 'active' voxels in these SPMs (statistical parametric maps) that are false positives. The SPMs from these individual analyses were used to generate a penetrance map. The penetrance map was constructed by using a look up table that colours the voxel according to how many of the three sites show a significant GM concentration change. In this way we can identify voxels in which all three individual site analyses show a significant GM concentration change at the specified threshold.

Across-site control analysis: Differences between sites were investigated by comparing control GM concentration images from the different sites using a voxel-wise two-sample *t*-test. These analyses were thresholded at $p < 0.05$ with FWE correction for multiple comparisons.

Combined site analysis: The GM concentration was modelled as a factorial design with site and epilepsy type (i. e. CAE and controls) as factors. By modelling the data in this way we were able to investigate the differences in GM distribution between CAE subjects and controls

after adjustment for inter-site differences in imaging equipment and acquisition parameters. The analysis was thresholded at $p < 0.05$ with family-wise error (FWE) correction for multiple comparisons. To test the impact of design balance on the VBM analysis, an analysis was undertaken with a reduced number of controls from Site A (33 controls). In order to examine the influence of smoothing kernel, the combined site analysis was repeated using 6mm and 16mm smoothing of the normalised, modulated GM segments. In order to test for the influence of the modulation step of optimised VBM, the analysis was repeated using normalised unmodulated GM segments smoothed with a 10mm FWHM Gaussian smoothing kernel. For the unmodulated VBM analysis, TIV was not included as a covariate due to the inherent correction for brain volume provided by spatial normalisation.

Thalamic GM concentration changes: The effect of site and CAE status on thalamic GM concentration was further investigated by creating a thalamic mask using the anatomical automated labeling toolbox (Tzourio-Mazoyer et al., 2002) and measuring the mean GM value in the thalamic mask from each beta (regressor) image representing the effect of interest (site and epilepsy status). A similar process was undertaken on the analysis in which data from all three sites was pooled together. Finally the mean change in thalamic GM concentration was calculated for the analysis in which site was included as a factor (analysis (ii) above) by measuring the mean GM value in the thalamic mask from a contrast image representing (a) controls from all three sites and (b) CAE subjects from all three sites. The standard error of the mean ($\sigma/\sqrt{n}$) associated with each measurement described in the previous paragraph was estimated by dividing the image representing the effect of interest by its corresponding test statistic image voxel-wise.

Variation of test statistic with sample size for single vs multi-site data—The value of including extra sites in the VBM analysis was investigated by measuring the test statistic in the thalamic region of interest as a function of the number of control subjects from site A. The test statistic was used as a metric to quantify the relative significance of the observed difference. The statistic was measured for four designs: (i) Site A alone, (ii) Site A + Site B, (iii) Site A + Site B + Site C, and (iv) Pooled data from all three sites (no site factor). In each case, only the number of Site A controls was varied (10–213 controls in 8 incremental steps, 1000 random samplings in each case).

Results

Individual site analyses

The individual site analyses show spatially heterogenous GM concentration changes when displayed at a lenient threshold ($p < 0.05$ uncorrected for multiple comparisons, Fig. 1). When a more stringent threshold is applied, such as the commonly used family-wise error correction ($p < 0.05$), no GM concentration changes are observed in the Site B and Site C analyses, presumably due to the low number of controls scanned at these sites compared to Site A. The penetrance map (Fig. 1, bottom row) indicates that the thalamic nuclei are the only regions that show GM concentration reduction in all three sites at the specified threshold.

Across-site control analysis

Comparisons of control data acquired from each site show significant putative GM concentration differences between sites (Fig. 2). The maps of GM concentration change are displayed at $p < 0.05$ with family-wise error (FWE) correction for multiple comparisons; therefore it can be seen that the across-site GM differences are significantly larger than the within-site GM differences associated with CAE (Fig. 1).

Combined site analysis

A voxel-based analysis of CAE subjects and controls from all three sites indicates that bilateral GM concentration decreases in the thalamic nuclei (Fig. 3). Site was explicitly included as a factor in the statistical model. The SPM in this case is presented at $p < 0.05$ with FWE correction. It can be seen that a considerably "cleaner" result is observed in the analysis in which site is included as a factor when compared with the individual site analyses. In order to investigate the influence of design balancing, a similar analysis was undertaken with a reduced number of controls from Site A (33 controls) to improve the ratio of controls to CAE subjects across sites and confirm that the Site A CAE/control differences are not biasing the final result. The Site A reduced controls analysis indicated similar patterns of reduced GM concentration in the CAE subjects, albeit at a lower threshold ($p < 0.001$ uncorrected for multiple comparisons).

Further VBM comparisons of CAE subjects and controls from all three sites were conducted using the unmodulated GM images with 10mm smoothing (without including TIV as a covariate), and different smoothing kernels (6mm and 16mm) on the modulated GM images. These analyses all gave similar patterns of GM reduction in the thalamic nuclei, with increased extent of the observed region of tissue change with an increased size of smoothing filter (images not shown). Qualitatively there was little difference between the implicated regions of change when comparing SPMs of modulated and unmodulated GM images.

Thalamic GM concentration changes

There is consistently decreased GM concentration in the thalamus of CAE subjects compared to controls for the data collected from each site (Fig. 4). These findings are consistent with the comparisons of CAE subjects with controls shown in Fig. 1. The plot also indicates systematic variation in thalamic GM concentration of controls between sites (black bars). This is consistent with the comparisons of control data from different sites shown in Fig. 2. The two bar plots on the right of Fig. 4 (labeled "grouped" on the horizontal axis) show the effect of pooling data from all three sites. It can be seen that if the data from all three sites is pooled, the mean GM concentration is similar in controls and CAE subjects; the consistent concentration reduction in CAE subjects is no longer observed.

Variation of test statistic with sample size for single vs multi-site data

It can be seen that above approximately 70 subjects (CAE and controls) the average Site A + Site B test statistic is greater than the average test statistic associated with the single Site A analyses (Fig. 5). Similarly if we extrapolate the Site A + Site B + Site C data we can see that above 70 subjects the average test statistic for the three site combined analysis would be greater than the single Site A analyses, and the Site A + Site B analyses. Finally it can be seen that if site is not included as a factor in the statistical analysis then the test statistic associated with the combined site data only approaches the single-site data when the total number of subjects in the study is approximately 220.

Discussion

We have demonstrated the feasibility of VBM analysis of images acquired at multiple sites imaged with different scanners (including different field strength) when the site is included as a factor in the statistical analysis of the acquired data. Explicitly modelling the site allowed differences between imaging sites to be separated from the disease effect of interest. The region that shows significant GM reduction in this combined analysis (thalamus, Fig. 3) is coincident with the region in which GM reduction is observed at a more lenient threshold in all three sites (Fig. 1, bottom row).

Our analysis indicates that there are significant regional GM variations in control MR scans acquired from different sites (Fig. 2). A likely explanation is that the measured gray-matter concentration, and the segmentation routines used to generate the GM concentration from the acquired images, are dependent on properties of the MR scanner, associated hardware and image acquisition parameters. A significant contribution to the observed differences in the thalamus between the 3T scanner and the 1.5T scanners (Fig. 2, top two rows) is probably due to different dielectric effects at these two field strengths, which manifest as a brighter signal at the centre of the brain at 3T (Tanenbaum, 2006). Variability in putative GM concentration across different scanners in the thalamic nuclei has been reported previously (Stonnington et al., 2008).

Our approach yielded significant results in the thalamic region even though Fig. 2 reveals that the between-site variation in this area is relatively large. The reason for this result is emphasised by the analysis shown in the bar plot in Fig. 4. The plot shows that there is consistently decreased GM concentration in the thalamus of CAE subjects at all three sites. This strongly suggests that this is a disease-specific finding. Although the effect is present in the disease data from all sites, it is swamped by the site-specific variation in this region when the data is simply pooled without modelling site effects.

By explicitly including the site as a factor in the statistical analysis the consistent differences in GM concentration between subject groups are retained. This means that our method can effectively separate the site variance from the disease variance. It is important to note that this approach requires *both* disease and control data from each site.

Fig. 5 indicates that there is a cross-over point between single-site analyses and multi-site analyses at approximately 70 subjects total. Below this point single-site analyses show, on average, a higher test statistic than multi-site analyses, indicating that the single-site analysis is more sensitive. Above this number the multi-site approach becomes the preferred methodology, presumably due to the inclusion of extra CAE subjects from other sites that outweighs the variance due to the extra sites.

It should be noted that the crossover at 70 subjects is specific to the number of controls and CAE subjects in our study and is also only determined by the effect size in the thalamic nuclei. Fig. 5 confirms that site must be included as a factor to maximise the sensitivity of the statistical analysis. When site is included as a factor the test statistic increases from 4.05 to 5.22 (all subjects included in analysis). Therefore it is not appropriate to simply pool data from all three sites without explicitly modelling site in the analysis. Whilst these findings are specific to this study, we believe that the existence of a cross-over point for which the multi-site approach becomes beneficial is generalisable. Future directions for investigating the feasibility of multi-site studies would include applying this type of analysis at the voxel level, as well as investigating different neurological disorders.

If we examine the epilepsy-specific contrasts in the VBM output, we see significant GM reduction in or close to the thalamic nuclei. These results are consistent with previous studies that implicate structural changes in the thalamic nuclei in the idiopathic generalised epilepsies, of which CAE is a sub-syndrome (Ciumas and Savic, 2006). VBM studies of other epilepsy syndromes, such as mesial temporal lobe epilepsy, have also indicated decreased GM concentration of the thalamic nuclei (McMillan et al., 2004; Mueller et al., 2006). Thalamic involvement has also been detected in fMRI studies of absence seizures (Salek-Haddadi et al., 2003).

Several methods have been proposed that may reduce the variability between images acquired on different scanners. Ideally the segmentation routines used in routine VBM analysis would generate tissue segments that are independent of the scanner used to acquire the data. Sequence-

independent tissue segmentation may be possible by integrating image acquisition parameters into the segmentation algorithms (Fischl et al., 2004). Processing of MR images prior to analysis using the voxel-based methodology, such as correcting for gradient non-linearities, has been shown to reduce voxel-wise intensity variability of MR scans of individuals rescanned on different scanners (Jovicich et al., 2006). Further research investigating analysis of cortical thickness measurements on MR images acquired at different sites has identified different field strength as the largest contribution to site-related within-subject variance (Han et al., 2006). The use of standardised image acquisition protocols for multi-site studies, such as those developed by the Biomedical Informatics Research Network (http://www.nbirn.net) and the Alzheimer's Disease Neuroimaging Initiative (Mueller et al., 2005), is also likely to help reduce voxel-wise variance in VBM analyses due to different imaging sites (Whitwell et al., 2007).

Whilst approaches such as these may substantially reduce differences between sites, we have demonstrated that a simple statistical adjustment provides adequate control over inter-site variability and allows us to combine data acquired at several sites for analysis using VBM. In MRI studies of diseases where only a limited number of subjects can be imaged at each site, our study supports the possibility of effective multi-site studies as long as disease subjects and healthy controls are acquired at every site.

Acknowledgments

This publication was supported by Program Grant 400121 from the National Health and Medical Research Council (NH&MRC), Australia, and Grant R37NS31146 (June 1, 2007–May 31, 2011) from NIH-NINDS, USA. The authors wish to acknowledge helpful contributions from the UCL Institute of Child Health, London, UK. The contents of this publication are solely the responsibility of the authors and do not necessarily represent the official views of the NH&MRC, NIH-NINDS or the UCL Institute of Child Health.

References

Berg AT, Shinnar S, Levy SR, Testa FM. Newly diagnosed epilepsy in children: presentation at diagnosis. Epilepsia 1999;40(4):445–452. [PubMed: 10219270]

Berg AT, Langfitt JT, Testa FM, Levy SR, Dimario F, Westerveld M, Kulas J. Global cognitive function in children with epilepsy: a community-based study. Epilepsia 2008;49(4):608–614. [PubMed: 18070088]

Chan CH, Briellmann RS, Pell GS, Scheffer IE, Abbott DF, Jackson GD. Thalamic atrophy in childhood absence epilepsy. Epilepsia 2006;47(2):399–405. [PubMed: 16499767]

Ciumas C, Savic I. Structural changes in patients with primary generalized tonic and clonic seizures. Neurology 2006;67(4):683–686. [PubMed: 16924024]

Fischl B, Salat DH, van der Kouwe AJW, Makris N, Segonne F, Quinn BT, Dale AM. Sequence-independent segmentation of magnetic resonance images. Neuroimage 2004;23(Supplement 1):S69. [PubMed: 15501102]

Good CD, Johnsrude IS, Ashburner J, Henson RN, Friston KJ, Frackowiak RS. A voxel-based morphometric study of ageing in 465 normal adult human brains. Neuroimage 2001;14(1 Pt 1):21–36. [PubMed: 11525331]

Han X, Jovicich J, Salat D, van der Kouwe A, Quinn B, Czanner S, Busa E, Pacheco J, Albert M, Killiany R, Maguire P, Rosas D, Makris N, Dale A, Dickerson B, Fischl B. Reliability of MRI-derived measurements of human cerebral cortical thickness: the effects of field strength, scanner upgrade and manufacturer. Neuroimage 2006;32(1):180–194. [PubMed: 16651008]

Jovicich J, Czanner S, Greve D, Haley E, van der Kouwe A, Gollub R, Kennedy D, Schmitt F, Brown G, Macfall J, Fischl B, Dale A. Reliability in multi-site structural MRI studies: effects of gradient non-linearity correction on phantom and human data. Neuroimage 2006;30(2):436–443. [PubMed: 16300968]

McMillan AB, Hermann BP, Johnson SC, Hansen RR, Seidenberg M, Meyerand ME. Voxel-based morphometry of unilateral temporal lobe epilepsy reveals abnormalities in cerebral white matter. Neuroimage 2004;23(1):167–174. [PubMed: 15325363]

Mueller SG, Weiner MW, Thal LJ, Petersen RC, Jack C, Jagust W, Trojanowski JQ, Toga AW, Beckett L. The Alzheimer's disease neuroimaging initiative. Neuroimaging Clin N Am 2005;15(4):869–877. xi–xii. [PubMed: 16443497]

Mueller SG, Laxer KD, Cashdollar N, Buckley S, Paul C, Weiner MW. Voxel-based optimized morphometry (VBM) of gray and white matter in temporal lobe epilepsy (TLE) with and without mesial temporal sclerosis. Epilepsia 2006;47(5):900–907. [PubMed: 16686655]

Proposal for revised classification of epilepsies and epileptic syndromes. Commission on Classification and Terminology of the International League Against Epilepsy. Epilepsia 30(4):389–399. [PubMed: 2502382]

Salek-Haddadi A, Lemieux L, Merschhemke M, Friston KJ, Duncan JS, Fish DR. Functional magnetic resonance imaging of human absence seizures. Ann Neurol 2003;53(5):663–667. [PubMed: 12731002]

Stonnington CM, Tan G, Kloppel S, Chu C, Draganski B, Jack CR Jr, Chen K, Ashburner J, Frackowiak RSJ. Interpreting scan data acquired from multiple scanners: A study with Alzheimer's disease. Neuroimage 2008;39(3):1180–1185. [PubMed: 18032068]

Tanenbaum LN. Clinical 3T MR Imaging: mastering the challenges. Magn reson imaging clin N Am 2006;14(1):1–15. [PubMed: 16530631]

Tzourio-Mazoyer N, Landeau B, Papathanassiou D, Crivello F, Etard O, Delcroix N, Mazoyer B, Joliot M. Automated anatomical labeling of activations in SPM using a macroscopic anatomical parcellation of the MNI MRI single-subject brain. Neuroimage 2002;15(1):273–289. [PubMed: 11771995]

Whitwell JL, Przybelski SA, Weigand SD, Knopman DS, Boeve BF, Petersen RC, Jack CR Jr. 3D maps from multiple MRI illustrate changing atrophy patterns as subjects progress from mild cognitive impairment to Alzheimer's disease. Brain 2007;130(7):1777–1786. [PubMed: 17533169]

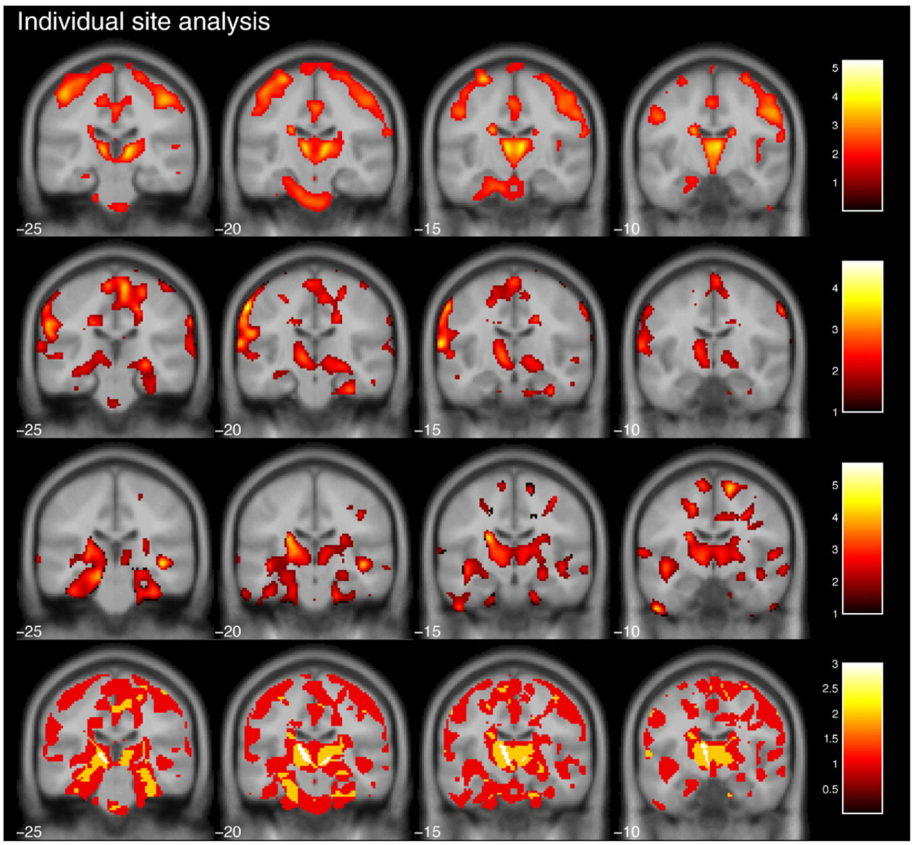

Fig. 1.

Regional GM concentration decrease in CAE compared to normal controls. The rows indicate an analysis of MR images acquired at different sites; 1st row Site A (3 T), 2nd row Site B (1.5 T), 3rd row Site C (1.5 T). The images are displayed at $p<0.05$ uncorrected for multiple comparisons. The bottom row is a penetrance map showing voxels common to all three sites (white), two sites (orange) or one site (red).

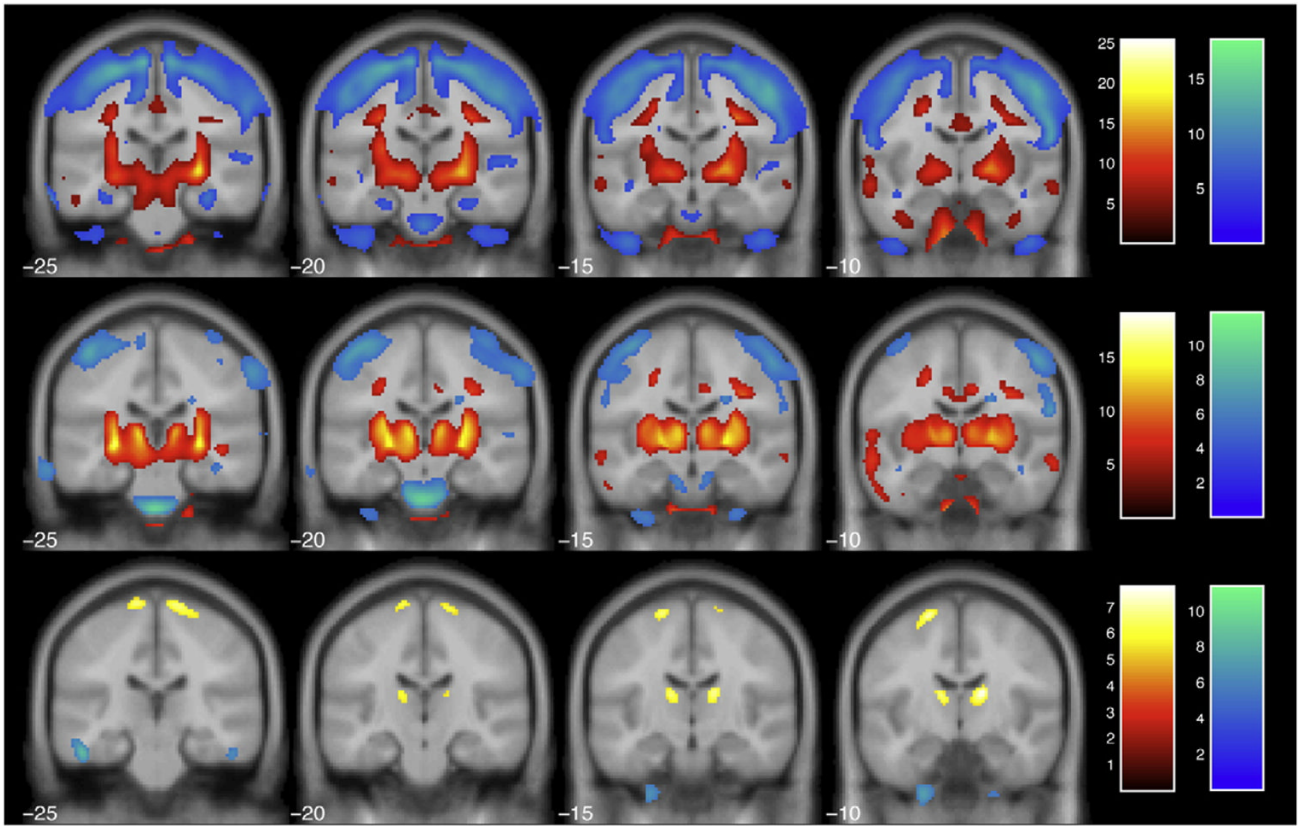

Fig. 2.

Comparison of putative differences in regional GM concentration of control groups between sites. Top row: GM tissue decreases in Site A compared to Site B ("hot" colour look up table), GM tissue increases in Site A compared to Site B ("winter" colour look up table). Middle row: GM tissue decreases in Site A compared to Site C (same colour scheme as top row). Bottom row: GM tissue decreases in Site B compared to Site C (same colour scheme as top row). The images are displayed at $p < 0.05$ (FWE correction).

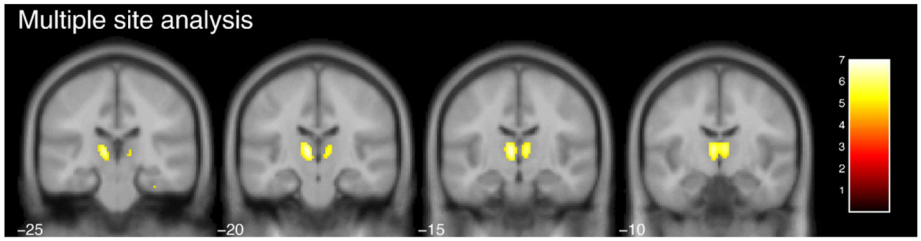

Fig. 3.
A factorial analysis of CAE and control data from all three sites in which site is included as a factor ($p<0.05$ FWE correction).

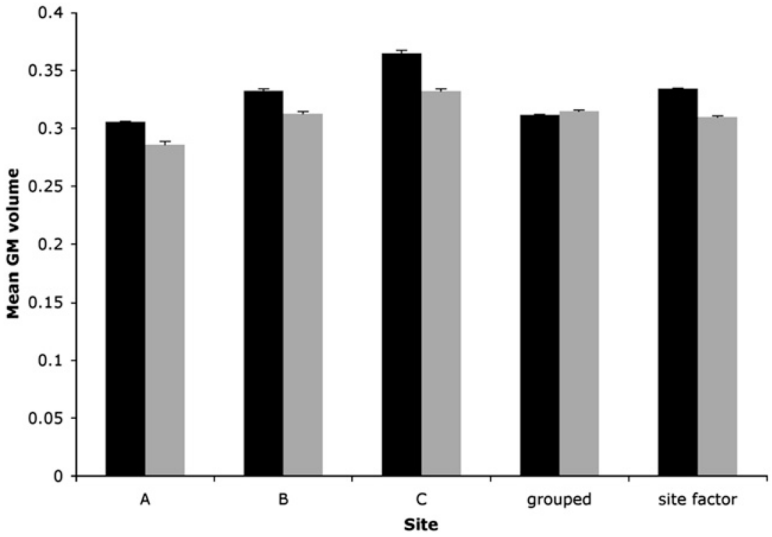

Fig. 4.

Average thalamic GM concentration in controls (solid black bars) and CAE subjects (gray bars) for each site, all data grouped together, and the same data in which site is included as a factor. The values on the vertical axis are a measure of the probability of being GM (a value of 1 indicates 100% GM). The error bars represent the standard error of the mean. Site A: 213 controls, 10 CAE subjects. Site B: 33 controls, 15 CAE subjects. Site C: 11 controls, 19 CAE subjects.

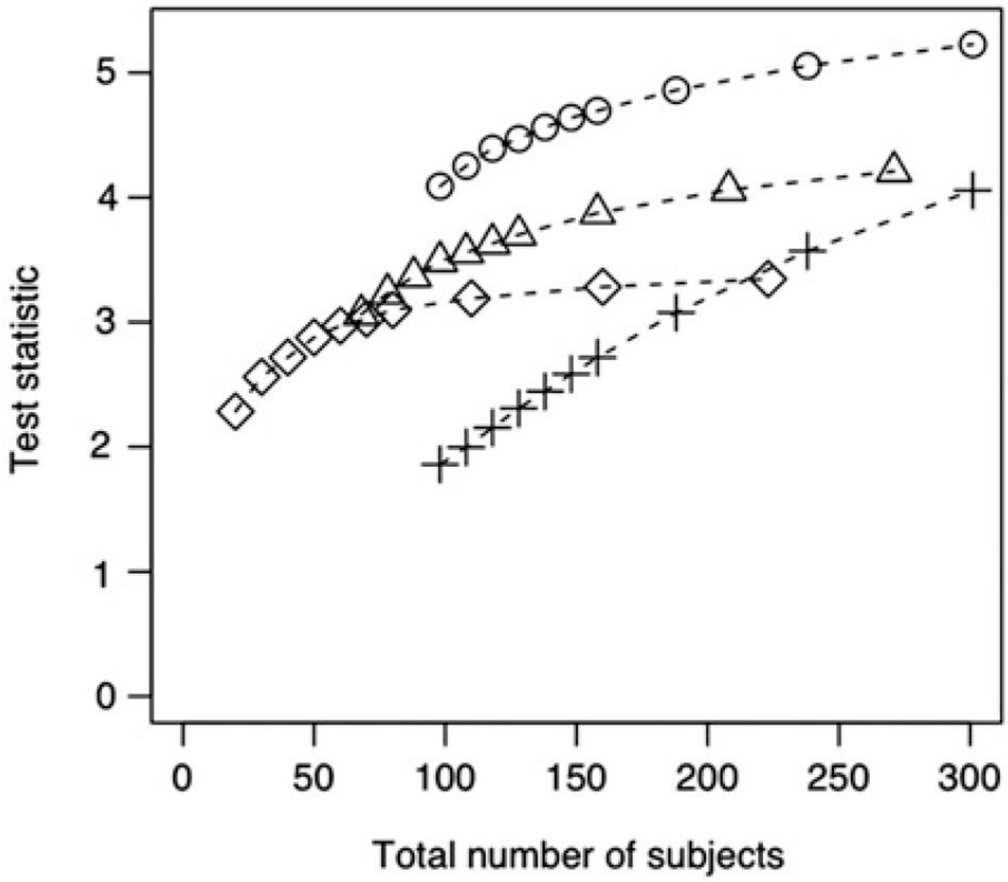

Fig. 5.

Variation of test statistic in thalamic GM with sample size in four designs. (i) Site A, diamond symbols, (ii) Site A+Site B, triangle symbols, (iii) Site A+Site B+Site C, circle symbols, and (iv) Pooled data (no site factor), cross symbol. In each case, only the number of site A controls was varied (1000 random samplings). The standard error on each value is negligible (range $0.023–8.14\times10^{-17}$) due to the number of resamplings. Site A data was using the single site because the large control group allowed for a more thorough investigation of the effect of control group size on the observed GM concentration in the thalamus.